

Investigation of Performance in Integrated Access and Backhaul Networks

Muhammad Nazmul Islam, Navid Abedini, Georg Hampel, Sundar Subramanian and Junyi Li
Qualcomm Flarion Technologies, Bridgewater, New Jersey

Abstract—Wireless backhaul allows densification of mobile networks without incurring additional fiber deployment cost. This, in turn, leads to high spatial reuse, which is a significant tool to meet increasing wireless demand in 5G networks. Integrated access and backhaul (IAB), where access and backhaul network share the same standard wireless technology (e.g. 5G new radio (NR) standard), allows interoperability among different IAB manufacturers and flexible operation between access and backhaul. This paper investigates joint resource allocation and relay selection in a multi-hop IAB network to maximize geometric mean of UE rates. Our study illustrates several advantages and features of IAB. First, IAB significantly improves UE rates compared to access only networks and can provide an important intermediate solution during incremental fiber deployment. Second, IAB networks with optimal mesh outperforms IAB networks with RSRP based spanning tree both in terms of rate and latency.

Keywords—Backhaul, Access, Relay, Integrated access and backhaul, Self-backhaul, 3GPP, 5G, New Radio.

I. INTRODUCTION

Wireless demand is expected to increase rapidly over the next few years. Higher bandwidth and spatial reuse are necessary to meet this increasing demand [1]. Due to the availability of abundant bandwidth and higher spatial reuse through directional beamforming, millimeter wave (MMW) bands (10 times the current carrier frequency of 3 GHz) can fulfill both of these criteria. That is why, millimeter wave based cellular access has been an integral part of LTE Rel-15 [2].

Signals transmitted via millimeter wave band, however, suffer from high path loss due to the use of higher carrier frequency and different additional propagation losses like oxygen absorption loss, rain absorption loss, etc. [3]. Hence, millimeter wave based cellular access is only feasible for small cell networks. Providing wired backhaul to many small cells may dramatically increase fiber deployment cost. Wireless backhaul allows network operators to flexibly deploy small cell base stations without incurring additional fiber deployment cost. Wireless backhaul is also an important tool during *incremental deployment* of fiber in mobile networks. During the early stages of a network rollout, fiber can be deployed to a subset of base stations, also known as anchor nodes, and the access traffic of the remaining base stations can be wirelessly backhauled to the anchor nodes. As network traffic demand grows, fiber can be deployed to all base stations of the network to further enhance capacity.

Wireless backhaul can be implemented using different techniques. Integrated access and backhaul (IAB), where access and backhaul communications use the same standard radio technology (e.g. 5G NR), allows interoperability among

base stations from different manufacturers, which is essential for flexible deployment of dense small cell networks [4]. IAB can be deployed through both in-band and out-band relaying and used in both indoor and outdoor networks. This paper investigates joint resource allocation and relay selection in a multi-hop IAB network to maximize geometric mean of UE rates. Our study illustrates several advantages and features of IAB.

A. Related Work

Several works have focused on resource allocation, relay selection and fiber deployment in wireless backhaul networks. The authors of [5]–[8] investigated optimal relay placement in backhaul networks to meet a certain demand at base stations. Rasekh et. al. [9] tackled the issue from the other direction, i.e., they performed joint resource allocation to maximize rate in a wireless backhaul network with a fixed set of anchor nodes.

The authors of [10] and [11] extended above works to IAB networks. Islam et. al. [10] performed joint optimal resource allocation, relay selection and fiber drop deployment to minimize the fiber deployment cost while meeting UE demand. It, however, did not illustrate UE rate distribution in various scenarios with fixed fiber deployment in the networks. Kulkarni et. al. [11] focused on an IAB based millimeter wave cellular network and investigated the performance of dynamic TDD networks with unsynchronized and access-backhaul split at different base stations. It constrained the maximum number of hops between UE and anchor nodes to be two and used Poisson point process based deployment of users and base stations to illustrate the rate distribution in IAB networks.

Compared to the above mentioned works, our work provides several novel findings. First, we use distribution of UE rates to show the advantages of IAB over purely access networks in a realistic multi-hop network setting of downtown Manhattan where the link gain between different nodes are obtained from a ray tracing tool. Second, we show that IAB can provide an important intermediate solution to increase UE rates during incremental fiber deployment. Third, we illustrate how the performance of an IAB network generated with signal-strength-based spanning tree topology compares with that of an IAB network generated with load-balanced mesh topology.

This paper is organized as follows. Section II formulates the general optimization problem. Section III and ?? describe different variants of the general optimization problem and the solution methodology respectively. After providing simulation results in section IV, we conclude our work in section V.

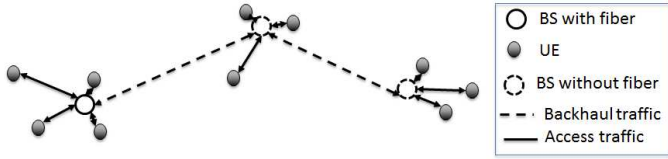


Fig. 1: A generic figure of integrated access backhaul network. Figure reproduced from [10]

Parameter	Notation
Set of user equipments	\mathcal{UE}
Set of base stations	\mathcal{BS}
Total number of UEs	N
Capacity of the fiber pipe	M
Allotted time in link ij for UL traffic	t_{ij}^U
Allotted time in link ij for DL traffic	t_{ij}^D
Flow in link ij for UL traffic	f_{ij}^U
Flow in link ij for DL traffic	f_{ij}^D
Capacity of link ij	c_{ij}
Available connectivity of access link ij	a_{ij}
Available connectivity of backhaul link ij	b_{ij}
fiber drop decision at BS j	y_j

TABLE I: List of Notations

Throughout this paper, the following terms may be used interchangeably, (“base station”, “BS” and “gNB”), (“user equipment” and “UE”), (“gNBs with fiber drop” and “anchor nodes”).

II. PROBLEM FORMULATION

Fig. 1 shows a generic integrated access backhaul network. Three base stations are connected to a group of UEs. Fiber is deployed in one base station. The other two base stations route their DL (UL) data from (to) the anchor node through one-hop and two-hop wireless backhaul paths.

Similar to this generic figure, we focus on a network with a set of UEs \mathcal{UE} and a set of base stations \mathcal{BS} . Our work maximizes the geometric mean (GM) of UE rates with a fixed set of fiber drops among the base stations.

Table I shows the list of parameters and the corresponding notations that we use throughout the paper. The variables are displayed with italic style in the table.

We now develop our optimization problem formulation by going through the set of constraints and optimization objective.

A. Objective

Let f_{ij}^D and f_{ij}^U denote the flow between node i and j to carry downlink (DL) and uplink (UL) traffic respectively. The geometric mean of all UEs’ rates can be expressed as:

$$\left(\prod_{i \in \mathcal{UE}} \left(\sum_{j \in \mathcal{BS}} f_{ij}^U \right) \left(\sum_{j \in \mathcal{BS}} f_{ji}^D \right) \right)^{\frac{1}{2N}} \quad (1)$$

The objective of the optimization problems considered in this paper is to maximize the above function.

B. Flow Capacity Constraint

Throughout this work, we assume that UEs always transmit at maximum power and the power spectral density does not depend on the allocated time duration. Hence, the flow of each link should be upper bounded by the product of the allocated time slots and the capacity of the link.

However, we also consider available connectivity pattern a_{ij} and b_{kl} for access link ij and backhaul link kl respectively. These available connectivity patterns are inputs to the optimization problem and determine whether the particular link can be activated or not. The specific values of these available connectivity patterns for different versions of the optimization problems are described in section III. Hence,

$$f_{ij}^U \leq t_{ij}^U c_{ij} a_{ij}, \quad f_{ji}^D \leq t_{ji}^D c_{ji} a_{ji} \quad \forall i \in \mathcal{UE}, \forall j \in \mathcal{BS}, \quad (2)$$

$$f_{ij}^U \leq t_{ij}^U c_{ij} b_{ij}, \quad f_{ji}^D \leq t_{ji}^D c_{ji} b_{ij} \quad \forall i \in \mathcal{BS}, \forall j \in \mathcal{BS}, i \neq j. \quad (3)$$

Note that, DL (UL) traffic in backhaul links refers to the portion of traffic that got generated from DL (UL) traffic in access links.

C. Flow Conservation Constraint

We set up the flow conservation constraint model in the same way as that of [10]. If a BS is not connected to fiber, outgoing and incoming flow should be equal. If a BS i is connected to fiber, summation of outgoing DL traffic in both access and backhaul should be less than the capacity of the fiber pipe at BS i . Similarly, summation of incoming UL traffic in both access and backhaul should not exceed the capacity of the fiber pipe at BS i . These relations can be expressed through the following constraints:

$$\sum_{l \in \mathcal{UE}} f_{il}^D + \sum_{j \in \mathcal{BS}, j \neq i} f_{ij}^D = \sum_{k \in \mathcal{BS}, k \neq i} f_{ki}^D + M_i^D \quad \forall i \in \mathcal{BS}, \quad (4)$$

$$\sum_{l \in \mathcal{UE}} f_{li}^U + \sum_{k \in \mathcal{BS}, k \neq i} f_{ki}^U = \sum_{j \in \mathcal{BS}, j \neq i} f_{ij}^U + M_i^U \quad \forall i \in \mathcal{BS}. \quad (5)$$

$$M_i^D + M_i^U \leq M y_i \quad \forall i \in \mathcal{BS}. \quad (6)$$

where M and y_i , inputs to the optimization problem, denote the total capacity of the fiber pipe and the fiber deployment decision at BS i respectively. M_i^D and M_i^U denote how BS i splits its total fiber capacity to carry DL and UL traffic respectively.

D. Resource Allocation Constraint

We assume time division multiplexing among adjacent links throughout this work and focus on in-band relaying where the partition between access and backhaul resources can vary across gNBs. Hence,

$$\sum_{i \in \mathcal{UE}} (t_{ij}^D + t_{ji}^U) + \sum_{k \in \mathcal{BS}} (t_{kj}^D + t_{kj}^U + t_{jk}^D + t_{jk}^U) \leq 1 \quad \forall j \in \mathcal{BS}, j \neq k \quad (7)$$

Our work can be easily extended to frequency division multiplexing based networks and out-band relaying techniques.

E. Interference Consideration

This paper focuses on IAB networks that operate at MMW band. Due to the directional transmission at MMW band, we do not assume interference among non-adjacent links and consider interference based IAB design as a future work. Our previous work [10] shows that pairwise interference from backhaul to access links exceed noise in only less than 7% cases in the network setting that we consider.

F. Overall Optimization Problem

$$\max \left(\prod_{i \in \mathcal{UE}} \left(\sum_{j \in \mathcal{BS}} f_{ij}^U \right) \left(\sum_{j \in \mathcal{BS}} f_{ji}^D \right) \right)^{\frac{1}{2N}} \quad (8a)$$

$$f_{ij}^U \leq t_{ij}^U c_{ij} a_{ij}, \quad f_{ji}^D \leq t_{ji}^D c_{ji} a_{ji} \quad \forall i \in \mathcal{UE}, \forall j \in \mathcal{BS} \quad (8b)$$

$$f_{ij}^U \leq t_{ij}^U c_{ij} b_{ij}, \quad f_{ji}^D \leq t_{ji}^D c_{ji} b_{ij} \quad \forall i \in \mathcal{BS}, \forall j \in \mathcal{BS}, i \neq j \quad (8c)$$

$$\sum_{l \in \mathcal{UE}} f_{il}^D + \sum_{j \in \mathcal{BS}, j \neq i} f_{ij}^D = \sum_{k \in \mathcal{BS}, k \neq i} f_{ki}^D + M_i^D, \quad \forall i \in \mathcal{BS} \quad (8d)$$

$$\sum_{l \in \mathcal{UE}} f_{li}^U + \sum_{k \in \mathcal{BS}, k \neq i} f_{ki}^U = \sum_{j \in \mathcal{BS}, j \neq i} f_{ij}^U + M_i^U, \quad \forall i \in \mathcal{BS} \quad (8e)$$

$$M_i^D + M_i^U \leq M y_i \quad \forall i \in \mathcal{BS} \quad (8f)$$

$$\sum_{i \in \mathcal{UE}} (t_{ij}^D + t_{ji}^U) + \sum_{k \in \mathcal{BS}} (t_{kj}^D + t_{kj}^U + t_{jk}^D + t_{jk}^U) \leq 1 \quad \forall j \in \mathcal{BS}, j \neq k \quad (8g)$$

$$f_{ij}^U \geq 0, \quad f_{ji}^D \geq 0, \quad t_{ij}^U \geq 0, \quad t_{ji}^D \geq 0 \quad \forall i \in \mathcal{UE}, \forall j \in \mathcal{BS}, \quad (8h)$$

$$f_{ij}^U \geq 0, \quad f_{ij}^D \geq 0, \quad t_{ij}^U \geq 0, \quad t_{ij}^D \geq 0 \quad \forall i \in \mathcal{BS}, \forall j \in \mathcal{BS}, i \neq j \quad (8i)$$

$$M_j^D \geq 0, \quad M_j^U \geq 0 \quad \forall j \in \mathcal{BS} \quad (8j)$$

We investigate different variants of the optimization problem mentioned above to see the impact of IAB networks. The next section describes these different variants.

III. DIFFERENT VARIANTS OF OPTIMIZATION PROBLEM

A. Access only, signal-strength-based cell selection

This scenario focuses on access only network, i.e., it does not allow any backhaul traffic. Hence, $b_{ij} = 0 \quad \forall i \in \mathcal{BS}, j \in \mathcal{BS}, j \neq i$. UEs are connected to the BS based on maximum signal strength. The possible access connectivity pattern is,

$$\forall i \in \mathcal{UE}, a_{ij} = 1 \text{ iff } c_{ij} \geq c_{ik} \quad \forall k \in \mathcal{BS}, k \neq j \quad (9)$$

Each UE is connected to only one BS. If, for a UE i , $c_{ij} = c_{ik} \geq c_{il} \quad \forall l \in \mathcal{BS}, l \neq j, l \neq k$, then one of a_{ij} and a_{ik} links gets randomly activated and the other remains inactive.

B. Access only, load-balanced cell selection

This scenario focuses on access only network, too. Hence, $b_{ij} = 0 \quad \forall i \in \mathcal{BS}, j \in \mathcal{BS}, j \neq i$. However, It allows any UE to be connected to any BS. Hence, $a_{ij} = 1 \quad \forall i \in \mathcal{UE}, j \in \mathcal{BS}$. One UE could be connected to multiple BSs in this scenario.



Fig. 2: A wireless network with 18 possible locations of base stations in downtown Manhattan. UEs are randomly distributed in streets and not shown in the figure

C. IAB, signal-strength-based cell selection and spanning tree (ST) topology

UEs are connected to BS based on maximum signal strength. Hence, the access connectivity is same as that of III-A. The backhaul connectivity pattern is generated using signal strength based spanning tree. The algorithm to generate the backhaul connectivity pattern can be described as follows:

- 1) Initialize the gNBs with fiber as connected nodes and gNBs without fiber as unconnected nodes.
- 2) Iterate through following steps till the set of unconnected nodes is an empty set.
- 3) Generate edge graph between the elements of the connected node set and those of the unconnected node set.
- 4) Pick the edge with the strongest link gain. Remove the corresponding unconnected node from the set of unconnected nodes and add it to the set of connected nodes. Go to step 2.

D. IAB, signal-strength-based cell selection and load-balanced mesh topology

UEs are connected to BS based on maximum signal strength. The access connectivity of this scenario is same as that of III-A. However, this scenario allows any base station to be connected with any other BS. Hence, $b_{ij} = 1 \quad \forall i \in \mathcal{BS}, j \in \mathcal{BS}, j \neq i$.

E. IAB, load-balanced cell selection and mesh topology

This scenario allows any UE to be connected to any BS and any base station to be connected with any other BS. Hence, $a_{ij} = 1 \quad \forall i \in \mathcal{UE}, j \in \mathcal{BS}$ and $b_{ij} = 1 \quad \forall i \in \mathcal{BS}, j \in \mathcal{BS}, j \neq i$. One UE could be connected to multiple BSs in this scenario.

IV. NUMERICAL SIMULATIONS

We consider a wireless network setting in downtown Manhattan and use it to show the usefulness of IAB networks. Fig. 2 shows the network location. The eighteen red circles denote possible locations for gNB deployment. The average

Parameter	Value
BS and UE Tx Power (dBm)	30
BS antenna array configuration	16×8
Array gain (dB)	21
BS EIRP (dBm)	51
Total bandwidth (GHz)	1
Frequency (GHz)	28
Atmospheric absorption (dB/km)	0.11
Polarization loss (dB)	1
Alignment error (dB)	5
Implementation loss (dB)	5
Capacity of fiber pipe (Gbps)	200

TABLE II: Link Budget Calculation

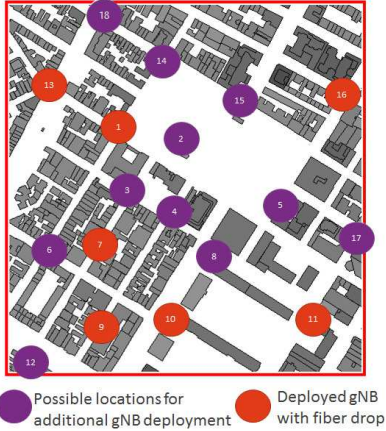


Fig. 3: The same wireless network of Fig. 2 where gNBs with fiber have been deployed in 7 out of the 18 possible deployment locations.

distance between these possible sites is 200 m. 600 UEs are randomly thrown into the open areas of the grid. The link gains between possible gNBs and UEs are obtained from WINPROP, a ray tracing tool [12].

We assume that each gNB has a rectangular planar array with 16×8 antenna elements. Each UE has only one antenna element. The transmit power at both gNB and UE is assumed to be 30 dBm. Our work can be easily extended to scenarios where BS and UE have different transmit powers. gNB uses constant phase offset beams and directs it towards the strongest cluster of the angle of arrival or departure of a particular link to communicate with a UE. The effective signal to noise ratio (SNR) of each link is modeled as the harmonic mean of the actual SNR and 30 dB. This limits the effective SNR within 30 dB. The minimum SNR of a link is assumed to be 0 dB, i.e., a link is assumed to exist only if the SNR of the link exceeds 0 dB. The capacity of each link is obtained using the effective SNR of the link, total bandwidth and Shannon's capacity theorem.

Table II lists the simulation parameters that we have used throughout this paper. The next several sub-sections describe simulation results illustrating the advantages and some features of IAB networks.

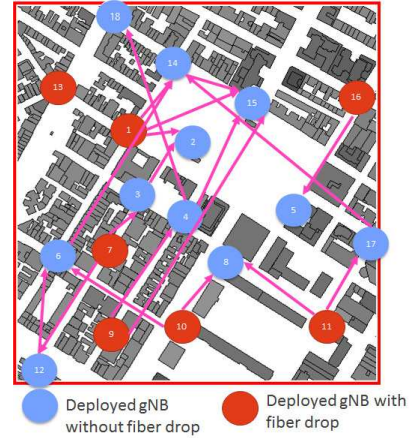


Fig. 4: Routing path of DL backhaul flow in the IAB network with signal-strength-based cell selection and load-balanced mesh topology

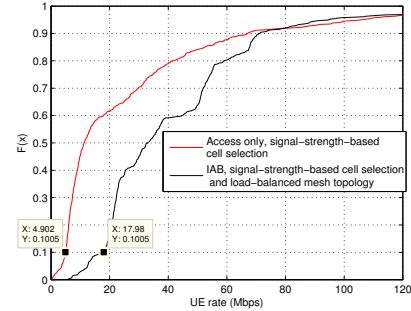


Fig. 5: UE rate distribution with IAB and access only networks with 7 fiber drops.

A. Comparison between IAB and access only network

We first select a set of gNBs as anchor nodes, i.e., as nodes with fiber deployment. This can be done randomly or using some metric. In this paper, we select the specific anchor nodes to minimize the total number of anchor nodes while meeting UEs' demands in an access only network. This part of our work was previously addressed in [10] and will be skipped here for brevity. Fig. 3 shows the location of the gNBs with fiber deployment. The UE locations are not shown in the figure. Based on the selected set of fiber deployment, we maximize the geometric mean of UE rates throughout the network and run different versions of the optimization problem that are described in section III. Fig. 4 shows the routing path for downlink flows between gNBs with fiber drop and gNBs without fiber drop in the IAB network with signal-strength-based cell selection and load-balanced mesh topology. The connectivity between UEs and gNBs are not shown in the figures throughout the paper. Fig. 5 shows the distribution of UE rates in both IAB networks and access only networks. These results were obtained using signal-strength-based cell selection. Fig. 5 shows that the top 10 percentile UEs obtain similar rates in both IAB and access only networks. However, IAB significantly increases the rate of bottom 90 percentile UEs.

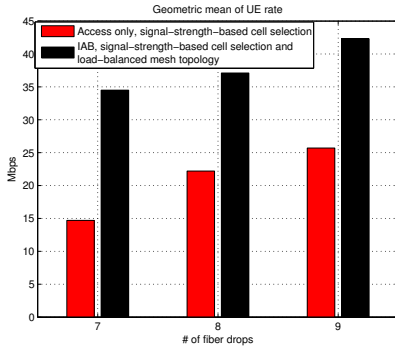


Fig. 6: Geometric mean of UE rates in IAB and access only networks for different number of fiber drops

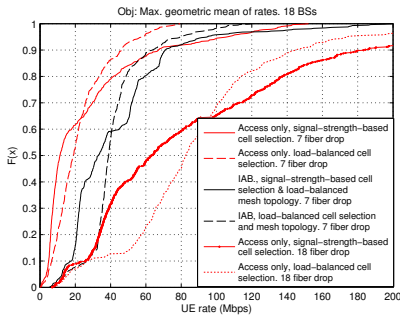


Fig. 7: Significance of IAB's role during incremental deployment in terms of UE rate

This result can be intuitively explained as follows: if cells are selected based on signal strength, UEs that are located close to gNBs with fiber drops will get similar rates in both IAB and access only networks. However, in access only networks, only 7 gNBs out of 18 possible site locations are connected to fiber drops. A lot of UEs get poor rates since they have to be attached with gNBs that are far from them. IAB, on the other hand, brings gNBs closer to the UEs while ensuring that fiber deployment cost remains the same. Hence, IAB allows network to significantly increase the rates of these 'far' UEs while retaining the rates of the 'near' ones. Fig. 6 shows the geometric mean of UE rates for different number of fiber drops. In the considered network setting, as long as the number of fiber drops is less than the total number of possible site locations, the geometric mean of UE rates in IAB networks remains greater than that of access only networks almost by a factor of 2.

B. Illustration of IAB's role in incremental fiber deployment

Fig. 7 and Table III show IAB's role in incremental fiber deployment. Results are shown for both signal-strength-based cell selection and load-balanced cell selection. As mentioned before, compared to access only networks having same number of fiber drops, IAB almost doubles geometric mean of UE rates. Deploying fiber to all site locations increases geometric mean of UE rates by another factor of 2. This shows that IAB can play a significant role during incremental fiber deployment.

Approach	GM of rate (Mbps)
Access only, signal-strength-based cell selection (7 fiber drops)	14.7
Access only, load-balanced cell selection (7 fiber drops)	17.5
IAB, signal-strength-based cell selection and load-balanced mesh topology (7 fiber drops)	34.5
IAB, load-balanced cell selection and mesh topology (7 fiber drops)	38.6
Access only, signal-strength-based cell selection (18 fiber drops)	64
Access only, load-balanced cell selection (18 fiber drops)	75

TABLE III: Geometric mean of UE rates in three scenarios: 1) access only network with 7 fiber drops, 2) IAB mesh network with 7 fiber drops and 3) access only network with 18 fiber drops.



Fig. 8: Routing path of DL backhaul flow in the IAB network with signal-strength-based cell selection and ST topology

Approach	GM of rate (Mbps)
Access only, signal-strength-based cell selection	14.7
IAB, signal-strength-based cell selection & ST topology	22.9
IAB, signal-strength-based cell selection & load-balanced mesh topology	34.5

TABLE IV: Comparison of geometric mean of UE rates among three scenarios: 1) Access only, 2) IAB with load-balanced mesh topology and 3) IAB with signal-strength-based ST topology

C. Comparison between IAB with load-balanced mesh topology and IAB with signal-strength-based spanning tree topology

We now investigate the performance of IAB networks with signal-strength-based spanning tree topology. Fig. 8 shows the routing pattern of the IAB network where the location of the fiber drop is same as that of Fig. 3. Since the backhaul connectivity pattern follows a spanning tree, each gNB without fiber is only connected to one gNB with fiber, potentially over multiple hops.

Fig. 9 and table IV compare the performance among access only network, IAB with load-balanced mesh topology and IAB with signal-strength-based spanning tree topology. IAB network with signal-strength based spanning tree topology

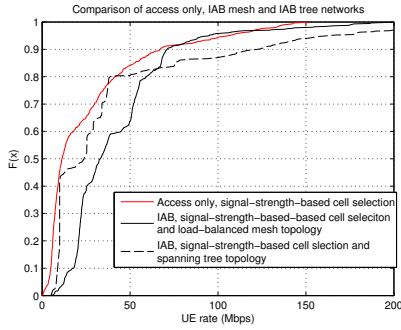


Fig. 9: UE rate distribution of IAB with load-balanced topology, IAB with signal-strength-based tree topology and access only networks with 7 fiber drops.

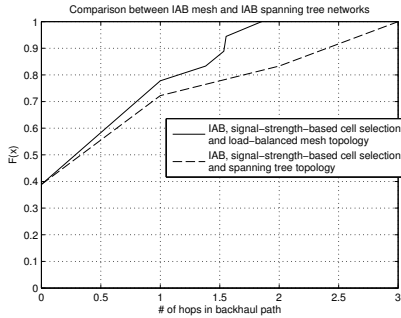


Fig. 10: Number of hops between gNBs and anchor nodes with IAB based on optimal mesh (generated using the routing pattern of Fig. 4) and IAB based on spanning tree (generated using the routing pattern of Fig. 8)

does not consider access load while connecting gNBs without fiber points with anchor nodes. As a result, some anchor nodes get connected to a lot of gNBs and UEs whereas some others get connected to only a few gNBs and UEs. Hence, the top 20 percentile UEs enjoy better rates in IAB with signal-strength-based spanning tree topology, but the bottom 80 percentile UEs enjoy better rates in IAB with load-balanced mesh topology. The geometric mean of UE rates of IAB network with signal-strength-based spanning tree topology lies between that of access only network and IAB network with load-balanced mesh topology.

Fig. 10 shows hop count distribution between gNBs and anchor nodes in both IAB scenarios. As shown in Fig. 4, a gNB may have multiple routes to its anchor(s) in an IAB network with load-balanced mesh topology. The hop count for these gNBs is determined as the rate-based mean value of the hop counts of its multiple routes.

Since there are 7 anchor nodes in the simulation setting, the number of hops for approximately 40% gNBs (7 out of 18) is zero in both IAB scenarios. Since IAB with signal-strength-based spanning tree does not consider access load while generating backhaul routing pattern, hop count in this scenario is significantly greater than that of IAB with optimal mesh networks. Hence, IAB with signal-strength-based spanning tree will suffer from higher latency as well.

V. CONCLUSION

Wireless backhaul increases both coverage and capacity in mobile networks and can play a crucial role during incremental deployment of fiber. IAB allows inter-operability among base stations from different manufacturers, which is essential for flexible deployment of dense small cell networks. This work investigates different aspects of IAB networks. Simulation results suggest that as long as the number of fiber drops is less than half of the total number of possible site locations, the geometric mean of UE rates in an IAB network remains almost a factor of 2 higher than that in an access only network. Besides, IAB network with signal strength based spanning tree topology performs worse than that with load-balanced mesh topology in terms of UE rate and latency. The performance of an IAB network with spanning tree can be improved by considering access load while generating the tree. Design and simulation of an optimal IAB network with access load and signal strength based spanning tree in MMW band remains an area of future work for our study.

REFERENCES

- [1] J. Andrews, "How can cellular networks handle 1000x data?" technical talk at University of Notre Dame. [Online]. Available: http://users.ece.utexas.edu/~bevans/courses/rtdsp/lectures/Andrews_Cellular1000x_N
- [2] 3GPP, "Study on channel model for frequency spectrum above 6 GHz," 38.900. version 14.3.1, Jul. 2017.
- [3] Z. Pi and F. Khan, "An introduction to millimeter-wave mobile broadband systems," *IEEE Communications Magazine*, vol. 49, pp. 101–107, 2011.
- [4] N. Abedini, M. N. Islam, G. Hampel, S. Subramanian, J. Cezanne, and J. Li, "Integrated access and backhaul in 5g - challenges and opportunities," in *IEEE mmSys (submitted)*, 2018.
- [5] G. E. O. A. Elgendy, M. H. Ismail, and K. Elsayed, "On the relay placement problem in a multi-cell lte-advanced system with co-channel interference," in *IEEE WiMob '2012*, 2012, pp. 159–165.
- [6] E. Karamad, R. S. Adve, and S. Guivarch, "Optimizing placements of backhaul hubs and orientations of antenna in small cell networks," in *IEEE BackNets 2015*, 2015.
- [7] M. N. Islam, A. Sampath, A. Maharshi, O. Koymen, and N. Mandayam, "Wireless backhaul node placement for small cell networks," in *IEEE CISS*, 2014.
- [8] B. Lin, P. Ho, L. Xie, and X. Shen, "Optimal relay station placement in IEEE 802.16j networks," 2007, pp. 25–30.
- [9] M. Rakesh, D. Guo, and U. Madhow, "Interference-aware routing and spectrum allocation for millimeter wave backhaul in urban picocells," in *IEEE ALERTON*, 2015.
- [10] M. N. Islam, S. Subramanian, and A. Sampath, "Integrated access backhaul in millimeter wave networks," in *IEEE WCNC*, 2017.
- [11] M. N. Kulkarni, J. G. Andrews, and A. Ghosh, "Performance of dynamic and static TDD in self-backhauled millimeter wave cellular networks," *IEEE Transactions on Wireless Communications*, vol. 16, pp. 6460–6478, 2017.
- [12] "WINPROP software kit," accessed February 2016, <http://www.awecommunications.com/Products/>.